Solar Energy 135 (2016) 750–757

Contents lists available at ScienceDirect

Solar Energy

journal homepage: www.elsevier.com/locate/solener

Optimum band gap combinations to make best use of new photovoltaic materials

S.P. Bremner [a,*], C. Yi [a], I. Almansouri [b], A. Ho-Baillie [a], M.A. Green [a]

[a] Australian Centre for Advanced Photovoltaics, School of Photovoltaic and Renewable Energy Engineering, University of New South Wales, Sydney 2052, Australia
[b] Department of Electrical Engineering and Computer Science, Masdar Institute, Abu Dhabi, United Arab Emirates

ARTICLE INFO

Article history:
Received 16 December 2015
Received in revised form 17 June 2016
Accepted 19 June 2016
Available online 29 June 2016

Keywords:
Active silicon substrate
Detailed balance
Limiting efficiency
Multi-junction solar cells

ABSTRACT

The detailed balance approach has been used to analyze the optimum use of band gaps in a multi-junction device of up to 6 sub-cells. Results for the AM1.5G spectrum suggest that as the number of sub-cells increases the importance of the bottom sub-cell band gap becomes less critical, assuming the optimum band gap combination for that value can be obtained. Given this greater freedom in choice, the potential for the use of silicon as an active substrate is investigated along with a cell thinning 'current sharing' approach to improve current mismatch in the device. Results show a more robust design space of multi-junctions with active silicon substrates when the current sharing approach is used, with performances close to the optimum for a completely free choice of band gaps. The use of the AM1.5D spectrum for a concentration ratio of 100, shows similar results for the substrate and a slight increase in band gap sensitivity for the upper band gaps in the stack. Inclusion of optical coupling between the sub-cells lowers limiting efficiency, with luminescent coupling mitigating the band gap sensitivity. The results and approach outlined are useful for determining how best to deploy new photovoltaic materials in multi-junction solar cells.

1. Introduction

Multi-junction (MJ) solar cells stand alone as the only successful strategy for boosting solar cell power conversion efficiencies above the single band gap detailed balance limit found originally by Shockley and Queisser (1961), with MJ limits being determined in the ensuing years (Henry, 1980; Marti and Araujo, 1996, Brown and Green, 2002, Bremner et al., 2008). By stacking different materials (with different band gaps) the photon energy above the band gap energy, which is lost in a single band gap device, can be harnessed more efficiently, leading to a high voltage device with a current that is reduced, but gives an improved overall performance. This relies on the MJ solar cell having the band gaps chosen in such a way as to minimize the potential current mismatch between the sub-cells in the stack. For the most common case of a monolithic MJ solar cell, where layers of different materials are grown on top of each other with a common substrate, a further restriction is designing to minimize the lattice mismatch between materials, to ensure material of sufficient crystalline quality for high photovoltaic performance.

In recent years impressive results focused on the lattice matched GaInP-Ga(In)As-Ge triad have led a renewed interest in the development of high efficiency multi-junction solar cells (Jones et al., 2012). Further to these successes, has been the development of devices using metamorphic step-graded alloy buffer layers (King et al., 2007; Geisz, 2008), which have delivered performances at the same level as the lattice matched approaches, with the latest generation of 'inverted' metamorphic devices (Geisz, 2008) holding the current champion efficiency (Soitec, 2014). For these metamorphic approaches the need for very close lattice matching is relaxed, meaning an ever expanding palette of different materials can now be investigated for high performance Photovoltaic applications. Reports of highly efficient materials such as Perovskites (Green, 2014; Petrović et al., 2015), lower cost CZTS (Shin et al., 2013) and even breakthroughs for more conventional III-V material growth on silicon (Grassman et al., 2013), point to a much greater choice of materials to be deployed in MJ solar cells.

The detailed balance limiting efficiency for photovoltaic energy converter designs offers insights into the relative performance of real devices against the ultimate performance permitted by the laws of physics. It allows for the potential of different materials as PV solar cells to be assessed not just for homo-junction devices, but also for multi-junction devices, where a combination of band gaps will be used. This is a crucial question to researchers investigating new PV

* Corresponding author.
E-mail address: spbremner@unsw.edu.au (S.P. Bremner).

http://dx.doi.org/10.1016/j.solener.2016.06.042
0038-092X/

materials systems: how can this material be used to greatest effect in a general PV device? As an example, most materials will not have the band gap to be ideal for a single band gap device, indeed any material with a band gap in excess of around 1.5 eV will most likely be best used in a MJ device as an upper sub-cell. But is it best suited to a three or four sub-cell MJ or for a MJ with an even greater number of sub-cells?

In this paper we report on detailed balance modelling of multi-junction solar cells under 1 sun AM1.5G and 100 suns AM1.5D spectra, to help guide how best to use a material in a high efficiency photovoltaic device. Our results show that the choice of band gap for the active substrate in a multi-junction device becomes less critical as the number of band gaps is increased, providing the optimum band gaps for the upper layers can be implemented. A general approach to deciding the best use of a new PV material is outlined and as an example the use of silicon as an active substrate for a three band gap multi-junction solar cell is detailed for the 1 sun AM1.5G spectrum case. We show that despite the optimal use of its band gap being as the middle sub-cell, the use of thinner upper layers to create a 'current sharing' arrangement sees the use of silicon as an active substrate perform well, with a relatively large design space.

2. Model used

A detailed balance model (Shockley and Queisser, 1961; Henry, 1980; Marti and Araujo, 1996, Bremner et al., 2008), was used to calculate all limiting efficiencies in this work. This means that all transitions considered balance exactly with their inverse at thermal equilibrium. It is assumed that for each sub-cell absorption is 100% of photons with energy greater than the sub-cell band gap, but lower than the band gap for the sub-cell immediately above, for the top cell this means effectively an infinite band gap (we set this to 5 eV). Light generated current values were evaluated using data for the AM15G spectrum given by the ASTM G-173 Reference Solar Spectrum Irradiance (IEC, 2008). The digitized data was used to calculate incremental power and photon numbers between successive values of wavelength, with these values kept in a Look Up Table (LUT). The total input power P_{IN}, which corresponds to the sum of all of the incremental powers, was calculated as a cross-check that the data was being calculated correctly. For each sub-cell band gap the equivalent wavelength was found, allowing the LUT to be referenced and the short circuit current to be found without additional calculations. The AM1.5G spectrum was used for 1 sun concentration results in all of the calculations presented. Calculations for concentrated sunlight are performed using this method in a straightforward manner using the AM1.5D spectrum.

It is further assumed that each sub-cell has a single chemical potential difference across it (that corresponds to the sub-cells operating voltage) and that the dark current for the sub-cells is given by the radiative emission of each sub-cell behaving as a modified Blackbody (BB). The emission flux of a sub-cell at a temperature, T, and with chemical potential difference, μ, given by the Bose–Einstein (BE) integral:

$$\phi(E_A, E_B, T, \mu, \Omega) = \frac{2\Omega}{h^3 c^2} \int_{E_A}^{E_B} \frac{E^2 dE}{\exp\left(\frac{E-\mu}{kT}\right) - 1} \quad (2)$$

for $0 < E_A < E_B$ and $\mu < E_A$. E_A and E_B are the energy limits of emission, and k is Boltzmann's constant. Ω is the étendue of the light emission, which is given by $\Omega = \pi n^2 \sin^2 \Theta_c$, where Θ_c is the half angle into which radiation can be emitted, and n is the refractive index of the medium light is being emitted into. As an example of finding the étendue, hemispherical emission into air ($n = 1$), such as a solar cell front surface emitting, means the étendue will be π. All of the light emission calculations done in this work assumed hemispherical emission. The BE integral was calculated using a rapid flux calculation technique based on Incomplete Riemann Zeta Integrals (IRZIs) previously shown to give greater speed and stability for these types of calculations (Bremner et al., 2008).

The efficiency was found for each combination of band gaps by first finding the open circuit voltage of each sub-cell and setting this as the upper limit for the chemical potential during subsequent calculations. Since the connection is series constrained, the light generated currents for each sub-cell was calculated, with the sub-cell with the lowest light generated current taken as a control sub-cell, since it is this sub-cell that will set the current through all of the sub-cells in the stack. The chemical potential across the control sub-cell, μ_{cont}, was ramped from zero to the open circuit voltage in steps of 1 mV, with the net current being calculated to give its operating point. The corresponding operating points for the other sub-cells in the stack was then calculated by finding the chemical potential across each sub-cell that gives the same net current as the control sub-cell. The sum of the chemical potentials across all of the sub-cells in the stack is thus found, and when multiplied by the net current in the stack, the output power found. The maximum power is updated for any increase with each increment of chemical potential allowing the maximum power output for a single band gap combination to be found. Finally, due to the non-continuous nature of the AM1.5 spectra, cycling through the band gap combinations was undertaken rather than using an optimizer.

3. Results and discussion

3.1. Free choice of band gaps

The palette of materials with potential use for photovoltaics is ever expanding, however, if one is restricting consideration to only a single band gap device, the suitability of a newly discovered material may be poor if its band gap is outside of the 1.0–1.5 eV range. Even if within this range there may be more value for using the new material as part of a multi-junction device, rather than as a single band gap solar cell. It therefore makes sense to have some idea of what band gaps are most useful for different numbers of band gaps in a multijunction stack.

To this end detailed balance calculations have been performed for different numbers of band gaps in a multijunction arrangement, with it assumed that each cell only emits through its front surface (and therefore the étendue is π). This corresponds to the rear of each cell having an idealized reflector that allows light below the band gap of the sub-cell in question to pass freely, but reflects 100% of the light that can be absorbed by the sub-cell in question. This situation represents the best efficiency that the multijunction stack can achieve (Rühle, 2016), since emission is minimized, while still allowing all sub-cells to access the solar spectrum efficiently.

A search of possible combinations of band gaps was undertaken for each number of band gaps in the multi-junction stack. For two, three, and four band gap stacks initial searches with resolutions of 0.01 eV were used, while for five and six band gap stacks a resolution of 0.02 eV was used. This was necessary due to the large number of band gap combinations to be searched in order to be certain the maxima were being captured correctly. Following the initial search a refined search limiting the search ranges was used with the digitised AM1.5G data resolution was used for the two, three and four sub-cell cases, a final resolution of 0.01 eV was used for the five and six sub-cell cases. The results of these searches are summarized graphically in Fig. 1 below. The color coding indicates the position in the stack for which the band gap is optimal. Note

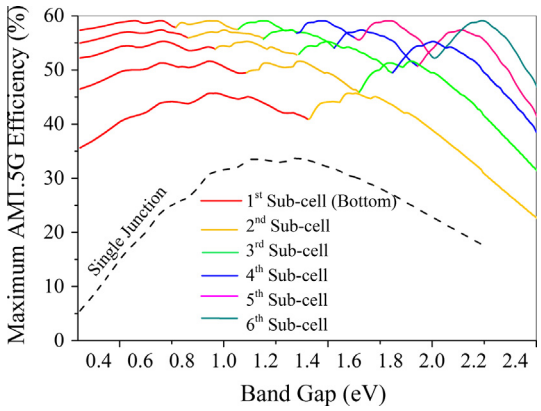

Fig. 1. Maximum efficiency for a band gap value as part of a multi-junction stack for cases up to and including six band gaps.

the maximum efficiency becomes less sensitive for lower sub-cells as the number in the stack increases.

There are some interesting features of these results. Firstly, great confidence in the results stems from observing that the peak efficiency value is repeated for each sub-cell range in each sub-cell number case. What this shows is that there is a single optimum band gap combination for each sub-cell number case, reading off the band gap values where the efficiency peaks will give the optimum combination. As an example when we read off the band gaps giving efficiency peaks for the 4 sub-cell case (0.71, 1.11, 1.49, 2.0 eV) agree with previous calculations (Brown and Green, 2002, Bremner et al., 2008).

We also see that there are at least two peaks for the bottom sub-cell band gap giving very similar peak efficiencies, a feature observed previously and which explains some of the disagreement on the optimum bottom band gap in earlier multi-junction calculations where optimizer routines were deployed (Bremner et al., 2008). In fact we see this type of feature in a number of the sub-cell ranges, suggesting the design space for MJs under AM1.5G should be explored with an optimizer cautiously as there are numerous local maxima that can give false universal maxima. It also means from a design point of view there is greater flexibility in the choice of band gap than might at first be thought. It is worth noting that while the bottom sub-cell band gap giving the global maximum in efficiency changes as the number of sub-cells increases, a substrate with a band gap in the 0.7–0.8 eV will always deliver a respectable performance with the maximum efficiency possible being at most a few absolute percent away from the global maximum (assuming the optimum band gap combination is achievable).

When we look at band gaps greater than around 1.4 eV, we see that for all of the cases calculated here a much greater sensitivity to the band gap combination is evident. Notable examples include ~1.72 eV where choosing this as the top most band gap in a two stack MJ solar cell is very close to optimum, but selecting it as either the middle or top sub-cell in a three stack MJ is the poorest choice available. For a band gap around 1.84 eV, this sort of effect is in evidence again, with this being an excellent choice for the top most band gap in a three stack MJ, but the poorest choice for either of the top most sub-cells in a four stack MJ, in fact its performance is worse than a significant part of the band gap range for the three stack top most sub-cell band gap. Other examples are evident for the MJ stacks with higher number of band gaps, so the lesson to be drawn is clear: care must be exercised in selecting the uppermost band gaps or a poor performance can result.

The final noticeable feature is that, for sub-cell numbers three and above, the variation in efficiency as the bottom sub-cell band gap varies, is only small, indicating the limiting efficiency is relatively insensitive to the bottom sub-cell band gap value. This effect spreads to include the next sub-cell for sub-cell number 4 and up. For $n = 6$ we see that the performance of the MJ stack also becomes insensitive to the band gap of the third from bottom sub-cell. So for the $n = 4$ and $n = 6$ cases we see that as long as we can get the top cells with the optimized band gaps we have a great deal of flexibility in the band gaps of the lower cells. It must be stressed that we still need to make sure the upper cells are optimized to the lower band gaps that we select, this point is illustrated when we plot the optimum band gaps along with the maximum efficiency for a three sub-cell MJ solar cell, as shown in Fig. 2.

There are three distinct regions corresponding to the band gap of interest's position in the stack, but within two of these regions, corresponding to the band gap of interest being the middle or top sub-cell, as the band gap increases so do the other two band gaps in the stack. There are some steps in these values, due to the piecewise continuous nature of the AM1.5 spectrum, but generally speaking the band gaps increase in step with each other. Within the region where the band gap of interest is the bottom sub-cell, we see clearly that the design and performance of the MJ stack is less sensitive to changes in this band gap value. This is an important result, since we are often concerned with what substrate to choose, these results indicate there is greater flexibility in choosing the upper band gaps than may first appear, and means materials concerns such as lattice constant and thermal expansion mismatch, miscibility gaps, as well as incompatible growth temperatures, can be the dominant factor in selecting materials to construct a multi-junction solar cell.

Crucially, as efforts to realize multi-junction solar cells with increasing numbers of sub-cells receives ever greater attention, these results indicate that the choice of lowest band gap and therefore the active substrate for a MJ solar cell is nowhere near as restrictive as may first be thought. In fact, provided we have the means to cover the higher band gap values required by our choice of bottom band gap, we may not have a completely free choice in substrate, but we are certainly not locked into one choice. This last observation leads to the commercially desirable choice of silicon as the active substrate for multi-junction solar cells, an area of increasing interest.

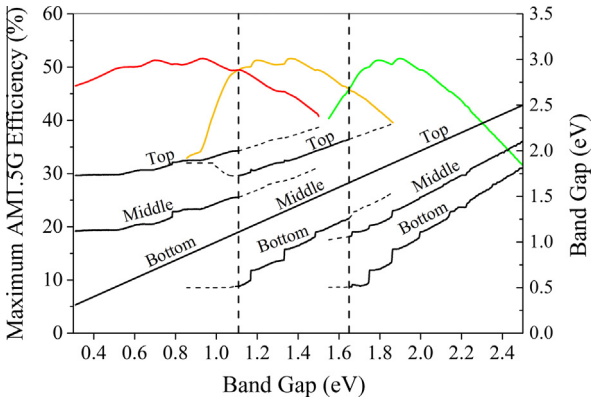

Fig. 2. Plot of maximum efficiency as band gap is varied, with the roll-off in efficiency included when the band gaps position in the stack is held beyond the crossover value, indicated by the vertical dashed lines. The solid black lines represent the band gaps for achieving maximum efficiency, with the dotted sections corresponding to the band gaps giving maximum efficiency for the stack position beyond the crossover value. Note there are step changes due to the piecewise continuous nature of the AM1.5 spectrum.

3.2. Impact of direct spectrum

The previous results are interesting from a design point of view, but MJ solar cells are often deployed in concentrator systems, to drive down cost per Watt. Since concentration will exclude the diffuse portion of the solar spectrum it therefore makes sense to look at any effects on the location of a band gap based on a modified, direct only spectrum such as AM1.5D. To this end, calculations were repeated for the case of three and four band gaps with the AM1.5D spectrum, and a concentration ratio of 100, with the results presented in Fig. 3 below.

Apart from the obvious increase in efficiency for both three and four sub-cell cases, it is noticeable in Fig. 3a that there is a larger sensitivity in efficiency when the band gap being varied is the uppermost in the MJ stack. Inspecting the region where the band gap is best used as a substrate it can be seen that a similar lack of sensitivity as in the AM1.5G case is repeated. The other slight difference with the AM1.5G case is that the crossover band gaps, where the optimum position in the MJ stack changes, are slightly lower. For instance in the 3 MJ case the substrate/middle sub-cell crossover has shifted from ~1.11 eV (AM1.5G) to ~1.03 eV (AM1.5D). When the optimum band gap combinations for the three sub-cell MJ stack under AM1.5D are plotted, as in Fig. 3b, similar results are given to the case of the three sub-cell MJ stack under AM1.5G.

This behavior can be understood by keeping in mind that the AM1.5D contains a lower proportion of power at the blue end of the spectrum. This is the main difference with the AM1.5G spectrum, and means that the losses due to thermalization of carriers for a band gap will be lowered for a given band gap relative to the AM1.5G case. This means lower band gaps are favored and this preference is seen in the cross-over band gaps displayed in Fig. 3a.

3.3. Optical and luminescent coupling between sub-cells

One further aspect to the MJ stack performance that can be explored is the impact of considering that the light emission by the sub-cells is influenced by the other sub-cells in the MJ stack. There are two aspects to this; firstly the light emission from a sub-cell is enhanced since the étendue depends on the refractive index of the medium that light is emitted into. This means the light emission at a particular chemical potential is enhanced by a factor of n^2 in comparison to the emission to air case considered in the previous sections. This light emission can also be through the front and the rear of the sub-cell, further increasing the emission by a particular sub-cell at a given chemical potential. The light emitted through the rear of a sub-cell can be absorbed by the sub-cell below it, adding to the current of that sub-cell. This second effect is referred to as luminescent (or radiative) coupling and has been explored in numerous publications (Friedman et al., 2013; Eisler et al., 2014; Friedman et al., 2014).

These effects were incorporated for the case of a three sub-cell MJ, with the refractive index of all sub-cells taken to be 3.4 to simplify the analysis (this is a 'typical' value for III-V materials like GaAs and silicon). The top cell has an étendue of π for its front surface and πn^2 for its rear surface, for the middle sub-cell front and rear etendue were both πn^2, finally the bottom sub-cell had a front etendue *of* πn^2 while the rear surface was assumed to have an ideal reflector (no rear emission).

The results of the calculations corresponding to the two cases highlighted are summarized in Fig. 4 below, with the results for the uncoupled AM1.5D 100× case included for comparison. It is clear that including the optical coupling significantly degrades performance across the entire band gap range out to roughly 2.0 eV. This makes complete sense since the light emission of each sub-cell (which corresponds to each sub-cells dark current) has been increased by a factor of 11.56 for each chemical potential. In effect the efficiency curve has been shifted downwards by approximately 4% absolute across the band gap range out to 2.0 eV, while the crossover band gaps have been pushed slightly higher. When the luminescent coupling is included it can be seen that performance is improved slightly and that the crossover band gaps have been lowered slightly to be back to the values found for the no coupling

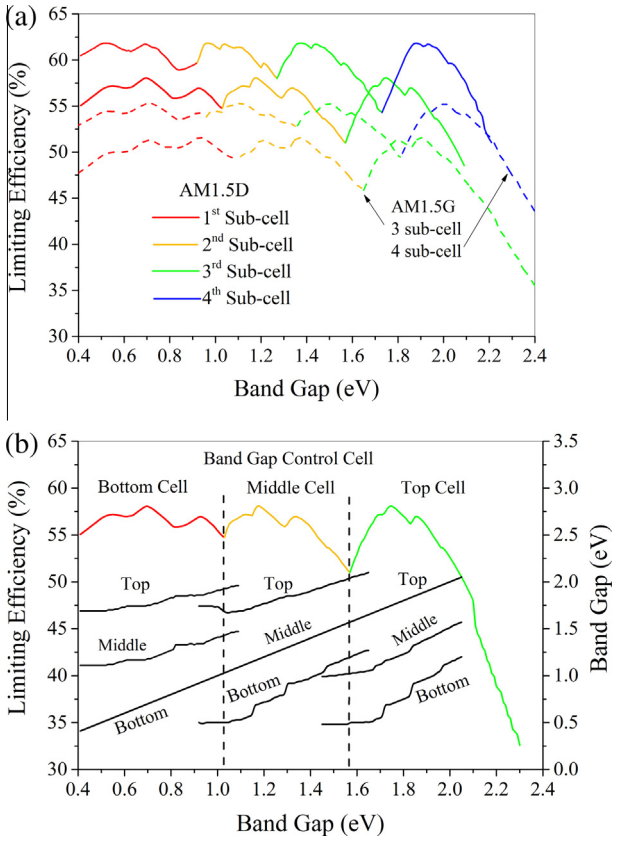

Fig. 3. (Top) Maximum limiting efficiency as a function of band gap for the case of three and four sub-cell multi-junction stacks under the AM1.5D spectrum and 100× concentration. The case for a three sub-cell stack under 1 sun AM1.5G spectrum is included for comparison. (Bottom) the optimum band gap combinations are plotted, showing the overlap regions around the crossover band gap values.

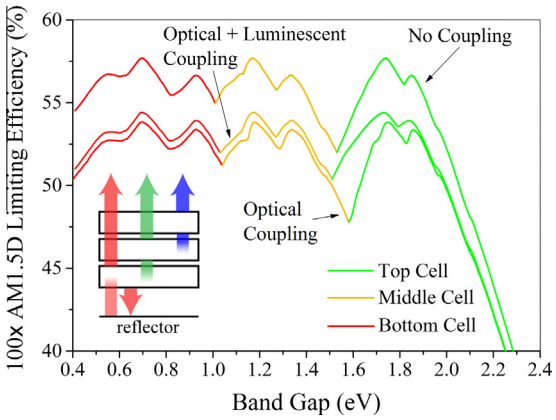

Fig. 4. Maximum limiting efficiency as a function of band gap for the case of the three sub-cell multi-junction stack under 100× AM1.5D with optical coupling between the sub-cells included, as well optical plus luminescent coupling between sub-cells (see inset for coupling case considered). The non-coupled three sub-cell stack case under 100× AM1.5D is included for comparison.

case. The most notable impact of including the luminescent coupling (apart from the increased efficiency) is the effect on the crossover band from middle to top sub-cell as the optimum position. Not only is the crossover band gap reduced, but the drop in efficiency, seen when using the AM1.5D spectrum, has been alleviated to be close to what was seen under the AM1.5G spectrum. This band gap de-sensitization has been reported previously (Eisler et al., 2014).

This behavior comes about because of the top and middle sub-cells acting as optical converters, absorbing a portion of the spectrum and then emitting light at its band gap wavelength. This emitted light then boosts the photocurrent of the sub-cell below, meaning a lower band gap for the sub-cell in question is favored, in order to minimize the current mismatch between sub-cells. It should be noted though that these effects are slight in terms of optimal band gap selection and that neglecting both the optical and luminescent coupling will in general still give an excellent guide as to how best to deploy a new PV material. Considerations of the coupling between sub-cells would be a fine tuning step in the design process with experimental results required to make physically relevant models (Friedman et al., 2013; Friedman et al., 2014).

3.4. Silicon as the active substrate

Silicon as the dominant commercial PV technology enjoys several significant advantages over other materials, even accounting for its relatively poor optical absorption. These include its low cost, incumbency in the microelectronics industry meaning it is extremely well characterized and a vast infrastructure for processing silicon devices is pre-existing. Traditionally this has not translated to the multi-junction solar cell field, where concerns such as lattice mismatch amongst other materials compatibility concerns have seen Germanium substrate designs dominate.

The concerns over lattice constant and thermal expansion coefficient mismatch lead to the need for thinner upper layers for a multi-junction to have the requisite material quality to deliver high performance. This means high radiative efficiency materials like III-V compounds are most favored. While a silicon substrate offers many cost and even mechanical strength advantages, the inability to grow high quality III-V materials on silicon precluded this potentially transformative technological development (Almansouri et al., 2015a, 2015b). Recent developments in growth techniques have once again opened up the possibility of realizing multi-junctions with active silicon substrates with III-V upper layers (Grassman et al., 2010) and more unconventional materials such as Perovskites (Green, 2014) and CZTS (Beiley and McGehee, 2012, Green et al., 2013). Assuming that high performing material can be deposited on silicon, and the silicon design can be optimized as part of the MJ stack (Almansouri et al., 2015a, 2015b), the most pressing question is then, what is the limiting performance of a MJ with silicon as the bottom cell?

As seen in Section 3.1 the band gap for the bottom sub-cell in a two stack MJ corresponds to silicon (~1.1 eV), a well-known result seen in many studies (Marti and Araujo, 1996, Brown and Green, 2002, Bremner et al., 2008). Of potentially more interest is the case of three sub-cells, where the band gap of silicon is not close to the optimum bottom sub-cell band gaps and is in fact close to the threshold for being better suited as the middle band gap in the stack. The question then is; what is the limiting performance of a three stack MJ with silicon as the active substrate?

In order to keep the analysis relatively simple, no coupling between sub-cells is assumed and light emission by the sub-cells is assumed to be to air and only through the front surface, as per Sections 3.1 and 3.2. It must be noted that inclusion of the effects of optical and luminescent coupling would alter the efficiencies found, as well as optimum band gap combinations, slightly, as seen in Section 3.3. Plotted in Fig. 5 is a contour plot of the three sub-cell limiting efficiency under 1 sun AM1.5G spectrum as the upper two band gaps are varied, with the bottom band gap fixed to 1.12 eV. As can be seen there is a 'window' in which we can achieve very respectable efficiencies, provided we can provide upper sub-cells within a triangle of values bounded at roughly 1.9 eV and 2.05 eV for the top band gap, 1.43 eV for the middle band gap, extending out to ~1.55 eV. Away from this region of band gap values the drop in performance when the top band gap is below 2.0 eV is precipitous. If the top band gap can be increased well beyond 2.0 eV then the drop in performance is not as drastic though undesirable.

Returning to Fig. 1 it can be seen that for the three sub-cell MJ the two bottom band gap peaks with highest efficiency are well away from the silicon band gap (~0.7 and 0.9 eV respectively). However, as noted earlier, the roll off in maximum efficiency away from the peaks is not excessive, but is still noticeable. In fact silicon's band gap is located where the band gap is ideal as the middle sub-cell, though it is close to the threshold between bottom and middle sub-cell being ideal. This would seem to argue against using silicon as the bottom sub-cell for a three stack MJ, but it is not a clear cut case since the drop off in efficiency from the global peak is not too oppressive (~2.5% absolute).

3.5. Current sharing

If we re-visit the assumptions made in these calculations it is not always the case that assuming 100% absorption in each layer delivers the best result for a given band gap combination. The reason is the current mismatch between different layers in the MJ, which is 'locked in' when we force 100% absorption in each layer. If the light generated current on offer to the MJ could be more evenly distributed then improved performance will ensue. This 'current sharing' approach consists of thinning upper layers in the stack to reduce light generated current, the photons that are deliberately not absorbed can then be absorbed by layers lower in the stack to balance the light generated currents in the MJ stack (Kurtz et al., 1990).

Current sharing will not work for all band gap combinations, but should be most effective when the upper layers in the MJ have the highest light generated currents in the stack. In the two sub-cell case the reasoning of when to apply a current sharing approach is essentially trivial since the silicon bottom sub-cell case gives the global maximum efficiency. This means a good current match exists, so if the band gap for the upper layer is below the optimum required, then a thinning can provide some improvement, but if

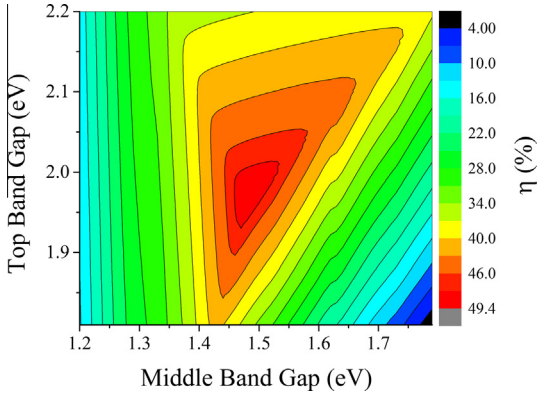

Fig. 5. Efficiency contour for a three sub-cell MJ solar cell with bottom sub-cell band of 1.12 eV, corresponding to a device with an active silicon substrate. As can be seen a relatively sharp drop-off in performance is seen away from the sweet spot when the top band gap lies below 2.05 eV.

greater than the optimum thinning the upper layer will only make the mismatch worse.

Displayed in Fig. 6 is a plot showing the magnitude of the greatest light generated current difference between the sub-cells in the stack, i.e. the maximal current mismatch in the stack. The dark jagged line passing from the bottom to the top of the plot marks the design space where the silicon bottom sub-cell is the current limiting cell in the stack (to the left of the line) and where either the top or middle sub-cells is the limiting sub-cell (to the right, no demarcation between the scenarios). This explains why Fig. 5 looks the way it does, essentially we are seeing the result of current mismatch between the sub-cells. This implies that minimizing this mismatch is the best way to improve performance, but the improvement is only expected in certain parts of the design space. The reason for this is that the strategy is most effective when the bottom silicon sub-cell is the lowest generating sub-cell in the stack, something that makes intuitive sense, since we can then tune the absorption of the upper layers to allow the optimum light

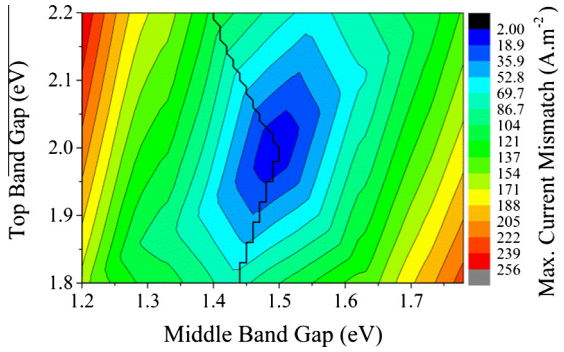

Fig. 6. Contour showing the maximum current mismatch between any of the sub-cells for the three sub-cell MJ case. To the left of the solid line is the design region in which the bottom silicon sub-cell has the lowest photocurrent in the MJ stack, to the right of the solid line either one of the middle or top sub-cells has the lowest photocurrent.

to reach the bottom sub-cell. For the situations when silicon is not the lowest generating sub-cell things become less clear, with a number of scenarios possible.

In terms of realizing this situation in our limiting efficiency calculations, for each combination of band gaps the light generated current of each sub-cell was calculated and then ranked. The rankings determined how the excess current in sub-cells would be divided between lower sub-cells. The assumption in these calculations is that a perfect match can be achieved i.e. we can set our layer thicknesses to deliver the exact level of absorption we require to balance light generated currents, when it is possible. Shown in Fig. 7 are the six different possibilities for the three sub-cell case, where for the cases shown as a–c, thinning of the sub-cells is expected to help improve efficiency. For the case d, the impact would be minimal, while for cases e and f there is no perceived benefit of applying thinning to the upper sub-cells. This approach was applied to each band gap combination and then the efficiency was calculated in the same manner as previously.

When we apply the current sharing approach to the limiting efficiency calculations the results are shown in Fig. 8 (Top), where it is immediately obvious that using this approach has expanded the design range in which high performance can be realized. This is an important point as it opens up a greater design space for MJs with active silicon substrates. Also shown in Fig. 8 (Bottom) is the change in absolute efficiency terms in comparison to the no current sharing, 100% absorption case typically calculated and displayed earlier in Fig. 5. This confirms that current sharing helps when the band gaps of the upper sub-cells are lower than optimum, but that when they are higher than optimum the impact is somewhat limited. Comparison of Fig. 8 (Bottom) with Fig. 6 shows that the current mismatch alleviation offered by current sharing is the sole cause for improvement and which light generated current ranking scenarios benefit most from current sharing.

3.6. Deciding how best to use a PV material

With the increasing discovery of more materials that can be deployed for photovoltaic applications a relevant question that

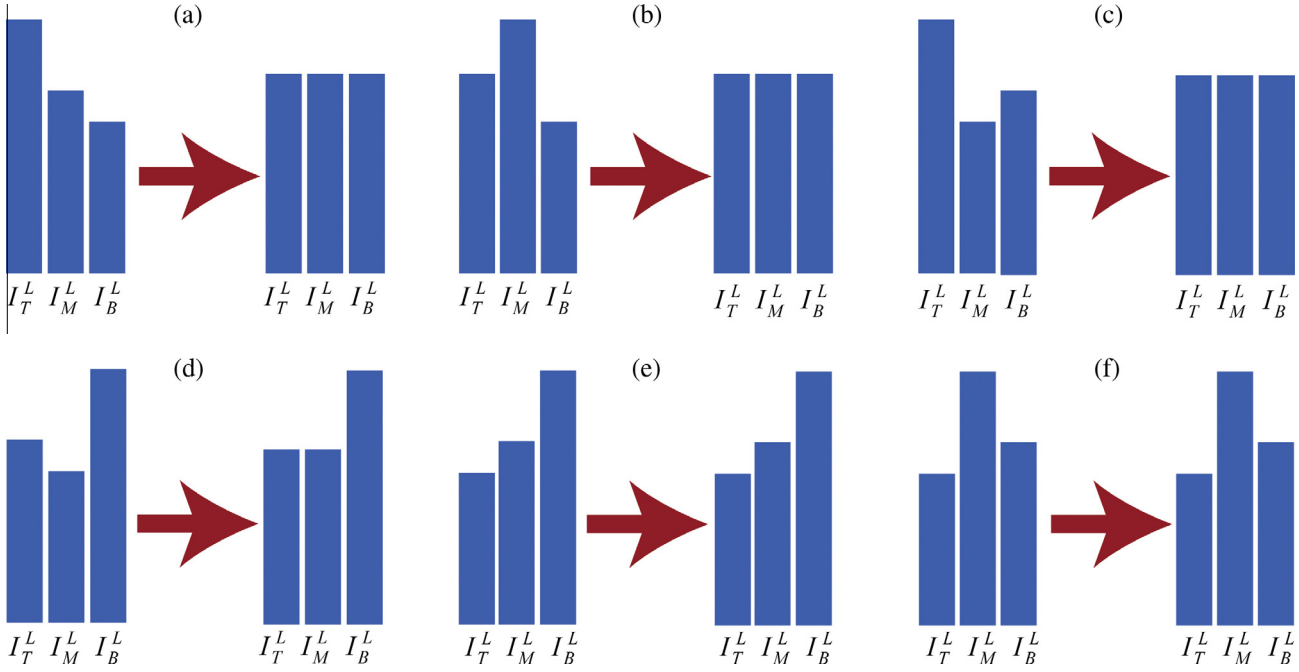

Fig. 7. Current sharing scenarios for the three sub-cell multi-junction stack case. The photocurrents for the sub-cells are ranked and then for cases where thinning of the upper cells will reduce current mismatch it is assumed that the thickness can be controlled to minimize mismatch.

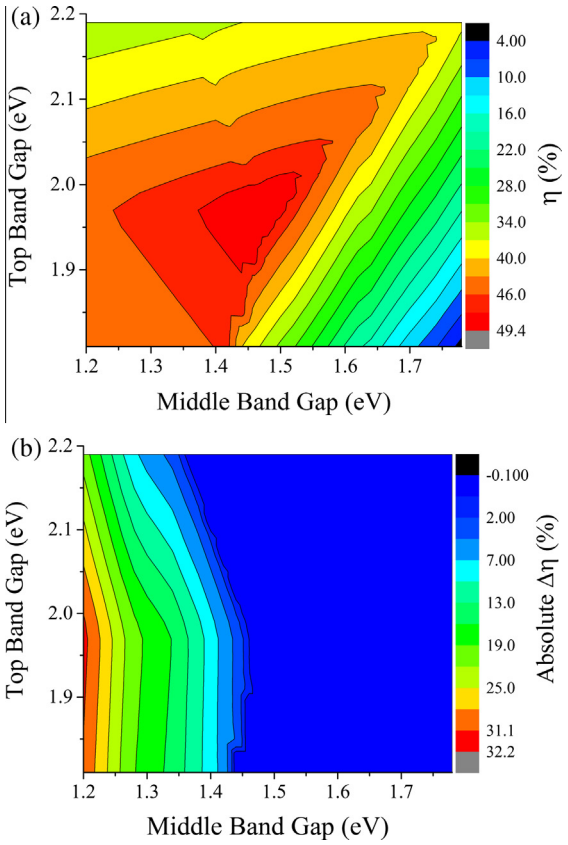

Fig. 8. (Top) Efficiency contour for three sub-cell MJ with current sharing in place, showing an expanded 'sweet spot' for the upper sub-cell band gaps, particularly for the middle band gap. (Bottom) shows the improvement in efficiency across the middle and upper band gap design space.

needs to be asked is how best to utilize the material. The number of materials with band gaps that will give optimum, or at least close to optimum, performance for a single band gap device is obviously limited. Besides, this is actually well covered with Si and GaAs, so there must be compelling reasons apart from limiting efficiency to choose a material over these two, particularly for silicon. This means if we are looking for high performance devices realized with new materials we are looking at MJ applications, in general. So figures like those presented in Figs. 1–4 are valuable first steps in deciding how best to use a new materials, particularly if concentration is being considered, but not the only step to follow. It has been seen that the inclusion of optical and luminescent coupling, detrimental for the ultimate attainable efficiency, but representing a more realistic scenario for monolithic MJs, has only a slight impact on the optimum location in a MJ stack for a particular band gap. Inclusion of luminescent coupling between the sub-cells limits the drop in efficiency seen near the middle/upper sub-cell crossover region for a three stack MJ under concentrated AM1.5D. This region would be avoided for real designs, so the impact of including coupling between sub-cells on any design process can be seen to be minimal for the initial limiting efficiency calculations. It must be stressed, however, that more refined designs after selection of materials systems would require these effects to be included as highlighted in a number of detailed studies on the effects of coupling on MJ device performance and design (Friedman et al., 2013; Friedman et al., 2014).

While this will give a good guide as to how best to deploy, further work must be done, particularly if, as was shown in the case of silicon as a bottom sub-cell, the band gap lies close to a threshold value where the band gaps optimum location in a MJ stack changes. Analysis of the expected light generated currents for a combination of band gaps that are perhaps recommended by lattice mismatch considerations can allow for current sharing approaches to improve performance further by minimizing current mismatch between sub-cells. This offers a relatively straightforward multi-stage procedure for determining the best way to utilize a new PV material.

4. Conclusions

We have presented results for the detailed balance limiting efficiency of multi-junction solar cells for up to 6 sub-cells under 1 sun AM1.5G and 100 suns AM1.5D spectrum. The impact of optical and luminescent coupling between sub-cells was also included for the 100 suns AM1.5D spectrum case. By conducting a large search of band gap combinations the best efficiency for a particular band gap regardless of its location in the MJ stack was determined and summarized graphically. It was found that the crossover band gap, where the optimum position that a band gap holds in a MJ stack changes, shifts to lower values with the removal of the diffuse component of the spectrum. Inclusion of optical coupling reduced efficiencies with a recovery seen by including luminescent coupling between sub-cells, which also has a very slight effect on crossover band gaps. The particular case of using silicon as an active bottom sub-cell under 1 sun AM1.5G spectrum was then explored with the three stack MJ being of great interest as the band gap of silicon is close to being best deployed as a bottom or middle sub-cell in the 3 cell stack. By current sharing, where upper layers are deliberately thinned to ensure much less than 100% absorption the design space available for the upper sub-cell band gaps was shown to be expanded, particularly, when the middle or the bottom cells are current limiting. Finally a process for determining how best to deploy a new PV material was surmised, with the need for further materials parameters like lattice constants being emphasized. With the proliferation of PV materials being reported in the literature this type of approach will be required in assessing the impact new materials can have.

Acknowledgements

This work was supported through The Australian Centre for Advanced Photovoltaics (ACAP), which encompasses the Australian-based activities of the Australia U.S. Institute for Advanced Photovoltaics (AUSIAPV) and is supported by the Australian Government through the Australian Renewable Energy Agency (ARENA).

References

Almansouri, I., Ho-Baillie, A., Bremner, S.P., Green, M.A., 2015a. Supercharging silicon solar cell performance by means of multijunction concept. IEEE J. Photovolt. 5 (3), 968–976.
Almansouri, I., Bremner, S.P., Ho-Baillie, A., Mehrvarz, H., Hao, X., Conibeer, G.J., Grassman, T.J., Carlin, J.A., Haas, A., Ringel, S.A., Green, M.A., 2015b. Designing bottom silicon solar cells for multijunction devices. IEEE J. Photovolt. 5 (2), 683–690.
Beiley, Z.N., McGehee, M.D., 2012. Modeling low cost hybrid tandem photovoltaics with the potential for efficiencies exceeding 20%. Energy Environ. Sci. 5, 9173.
Bremner, S.P., Levy, M.Y., Honsberg, C.B., 2008. Analysis of tandem solar cell efficiencies under AM1.5G spectrum using a rapid flux calculation method. Prog. Photovolt. Res. Appl. 16 (3), 37–45.
Brown, A.S., Green, M.A., 2002. Detailed balance limit for the series constrained two terminal tandem solar cell. Physica E 14, 96–100.
Eisler, C.N., Abrams, Z.R., Sheldon, M.T., Zhang, X., Atwater, H.A., 2014. Multijunction solar cell efficiencies: effect of spectral window, optical environment and radiative coupling. Energy Environ. Sci. 7, 3600–3605.
Friedman, D.J., Geisz, J.F., Steiner, M.A., 2013. Analysis of multijunction solar cell current-voltage characteristics in the presence of luminescent coupling. IEEE J. Photovolt. 3 (4), 1429–1436.
Friedman, D.J., Geisz, J.F., Steiner, M.A., 2014. Effect of luminescent coupling on the optimal design of multijunction solar cells. IEEE J. Photovolt. 4 (3), 986–990.

Geisz, J.F., Friedman, D.J., Ward, J.S., Duda, A., Olavarria, W.J., Moriarty, T.E., Kiehl, J. T., Romero, M.J., Norman, A.G., Jones, K.M., 2008. 40.8% efficient inverted triple-junction solar cell with two independently metamorphic junctions. Appl. Phys. Lett. 93, 123505.

Grassman, T.J., Carlin, J.A., Galiana, B., Yang, L.-M., Yang, F., Mills, M.J., Ringel, S.A., 2013. Nucleation-related defect-free GaP/Si(100) heteroepitaxy via metal-organic chemical vapor deposition. Appl. Phys. Lett. 102.

Grassman, T.J., Brenner, M.R., Gonzalez, M., Carlin, A.M., Unocic, R.R., Dehoff, R.R., Mills, M.J., Ringel, S.A., 2010. Characterization of metamorphic GaAsP/Si materials and devices for photovoltaic applications. IEEE Trans. Electron Devices 57 (10), 3361–3369.

Green, M.A., 2014. Perovskite single-junction and silicon- or CIGS-based tandem solar cells: hype or hope? In: 29th EU Photovoltaic Solar Energy Conference.

Green, M.A., Hao, X., Bremner, S.P., Conibeer, G.J., Al Mansouri, I., Song, N., Liu, Z., Ringel, S.A., Carlin, J.A., Grassman, T.J., Galiana, B., Carlin, A.M., Ratcliff, C., Chmielewski, D., Yang, L., Mills, M.J., Teeter, G., Young, M., 2013. Silicon wafer-based tandem cells: the ultimate photovoltaic solution? In: 28th EU Photovoltaic Solar Energy Conference.

Henry, C.H., 1980. Limiting efficiencies of ideal single and multiple energy gap terrestrial solar cells. J. Appl. Phys. 51 (8), 4494–4500.

IEC, 2008. International Standard. IEC 60904-3, Second ed. Photovoltaic Devices Part 3: Measurement Principles for Terrestrial Photovoltaic (PV) Solar Devices with Reference Spectral Irradiance Data. International Electrotechnical Committee (ISBN 2-8318-9705-X).

Jones, R.K., Ermer, J.K., Fetzer, C.M., King, R.R., 2012. Evolution of multijunction solar technology for concentrating photovoltaics. Jpn. J. Appl. Phys. 51, 10ND01.

King, R.R., Law, D.C., Edmondson, K.M., Fetzer, C.M., Kinsey, G.S., Yoon, H., Sherif, R. A., Karam, N.H., 2007. 40% efficient metamorphic GaInP/GaInAs/Ge multijunction solar cells. Appl. Phys. Lett. 90 (18), 2734507.

Kurtz, S.R., Faine, P., Olson, J.M., 1990. Modeling of two-junction, series-connected tandem solar cells using top-cell thickness as an adjustable parameter. J. Appl. Phys. 68 (4), 1890–1895.

Marti, A., Araujo, G.L., 1996. Limiting efficiencies for photovoltaic energy conversion in multigap systems. Sol. Energy Mater. Sol. Cells 43, 203–222.

Petrović, M., Chellappan, V., Ramakrishna, S., 2015. Perovskits: solar cells and engineering applications – materials and device development. Sol. Energy 122, 678–699.

Rühle, S., 2016. Tabulated values of the Shockley–Queisser limit for single junction solar cells. Sol. Energy 130, 139–147.

Shin, B., Gunawan, O., Zhu, Y., Bojarczuk, N.A., Chey, S.J., Guha, S., 2013. Thin film solar cell with 8.4% power conversion efficiency using an earth-abundant Cu_2ZnSnS_4 absorber. Prog. Photovolt. Res. Appl. 21, 72–76.

Shockley, W., Queisser, H.J., 1961. Detailed balance limit of efficiency of *p-n* junction solar cells. J. Appl. Phys. 32 (3), 510–519.

Soitec, 2014. Press Release. Fraunhofer Institute for Solar Energy Systems, 1 December 2014 (accessed at <http://www.ise.fraunhofer.de/en/press-and-media/press-releases/press-releases-2014/new-world-record-for-solar-cell-efficiency-at-46-percent> on 7 December 2014).